



Research article

UDC 552.111:550.4 (470.21)

Magma feeding paleochannel in the Monchegorsk ore region: geochemistry, isotope U-Pb and Sm-Nd analysis (Kola region, Russia)

Valeriy F. SMOLKIN¹✉, Artem V. MOKRUSHIN², Tamara B. BAYANOVA², Pavel A. SEROV², Aleksey A. ARISKIN³

¹ Vernadsky State Geological Museum, Russian Academy of Sciences, Moscow, Russia

² Geological Institute of the Kola Science Centre, Russian Academy of Sciences, Apatity, Russia

³ Lomonosov Moscow State University, Moscow, Russia

How to cite this article: Smolkin V.F., Mokrushin A.V., Bayanova T.B., Serov P.A., Ariskin A.A. Magma feeding paleochannel in the Monchegorsk ore region: geochemistry, isotope U-Pb and Sm-Nd analysis (Kola region, Russia). *Journal of Mining Institute*. 2022. Vol. 255, p. 405-418. DOI: 10.31897/PMI.2022.48

Abstract. A comprehensive study of a 340 m thick lenticular-sheet body of ultramafic composition penetrated by structural well M-1 at a depth of about 2.2 km was accomplished. Its main volume is composed of plagioclase-bearing rocks; fine-grained rocks of norite and orthopyroxenite chilling zones are preserved on endocontacts. The rocks of the body are similar in composition to the rocks near the underlying ore-bearing layered intrusion – the Monchepluton. The age of intrusion of the ultramafic body is 2510 ± 9 Ma (U-Pb, ID-TIMS, zircon) and, taking into account analytical errors, is comparable with the formation period of the Monchepluton (2507-2498 Ma). According to the study of the Sm-Nd system in rocks and minerals, a positive value of the ϵ_{Nd} (+1.1) parameter was established, similar to that in dunites and chromitites of the Monchepluton. Based on these results, the ultramafic body penetrated at depth was assigned to the magma feeding paleochannel through which the ultramafic, weakly contaminated magma entered the overlying magma chamber. This body is a unique example of a magma-feeding system for the ore-bearing layered intrusion of Precambrian age.

Keywords: Kola region; Paleoproterozoic; layered intrusions; gabbro-anorthosites; Monchepluton; Monchetundra massif; geochemical analysis; isotopic U-Pb and Sm-Nd systems

Acknowledgments. The research was carried out under the research programs 0226-2019-0053 and the grant of the Russian Science Foundation N 21-17-00161.

Received: 11.04.2022

Accepted: 15.06.2022

Online: 26.07.2022

Published: 26.07.2022

Introduction. Paleoproterozoic layered intrusions composed of mafic and ultramafic rocks are widespread in the Kola-Lapland-Karelian province, the most ancient part of the Fennoscandian Shield [1, 2]. One of the test sites for the study of layered intrusions was the Monchegorsk ore region lying in the central Kola region (Fig.1).

Layered ore-bearing intrusions of two age groups occur in the Monchegorsk ore region – the Monchepluton (2.50 Ga), Imandra-Umbarechinsky complex (2.44 Ga), coeval massifs of the largest gabbro-anorthosite complex of the Main Range as well as the deposits and ore occurrences of sulfide Cu-Ni-PGE, low-sulfide platinum-metal, chromite and titanomagnetite ores confined to them. A good exposure and accessibility of the territory are also important.

In the central part of the Monchegorsk ore region, a 2.5 km deep structural well M-1 was drilled for detecting ore bodies (Fig.1). At a depth of 2037-2377 m, the well crossed the ultrabasic body which is considered to be a magma feeding channel. Earlier, such channels were virtually unknown in the Precambrian layered intrusions. However, they are very important for solving the problem of magma intrusion mechanism and its intrachamber crystallization. This paper presents the results of the studies aimed at solving the problem of channels through which magma could enter the overlying magma chambers. The studies included geochemical, mineralogical, and isotope geochemical

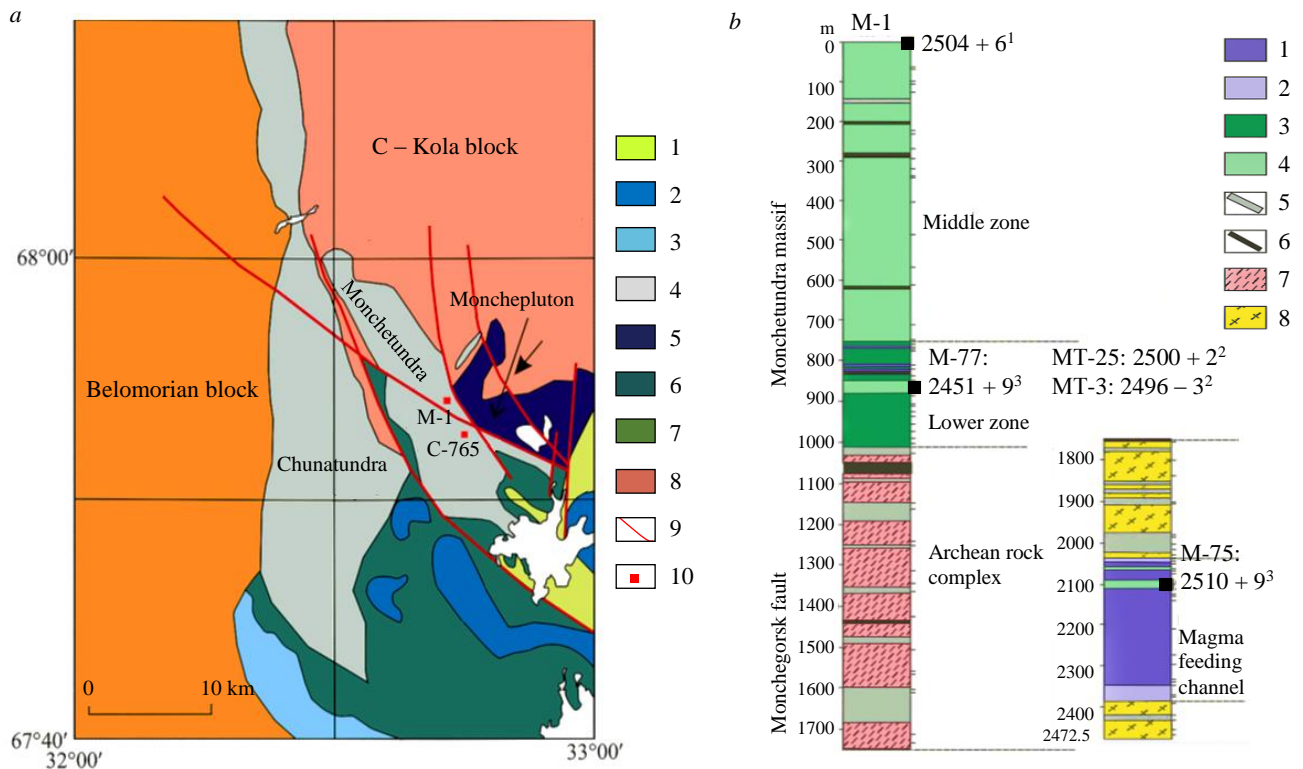


Fig.1. Scheme of geological structure of the Monchegorsk ore region (a) and section of structural well M-1 with indication of sampling sites and U-Pb zircon datings (b)

- a: 1 – sedimentary volcanic rocks of Imandra-Varzuga zone (<2.44 Ga); 2 – norite-gabbro-norites of Imandra-Umbarechensky complex (2.44 Ga); 3 – gabbroids of Nyark-tundra; 4 – gabbro-anorthosites of the Main Range (2.51-2.47 Ga); 5 – basic-ultrabasic rock of the Monchepluton (2.50 Ga); 6 – amphibolites of the Late Archean greenstone belt; 7 – tonalitic gneisses, amphibolites and migmatites of Belomorian megablock (>2.80 Ga); 8 – granites, diorites, aluminous gneisses, ferruginous quartzites of the Central Kola megablock (2.83-2.70 Ga); 9 – tectonic faults; 10 – location of wells M-1, C-765;
- b: 1 – plagiogabbros; 2 – orthopyroxenites; 3 – melanonorites; 4 – gabbro-norites, gabbro-anorthosites, gabbro-pegmatites; 5 – dikes of harrisites, gabbro-norites, microgabbro, granophyres; 6 – dolerite dikes; 7, 8 – complexes of plagiogneisses (7) and hypersthene diorites (8) and blastocataclases after them in the fault zone; 2504 ± 6 is the U-Pb isotope age of zircon (Ma): ¹ [3], ² [4], ³ the present work

(U-Pb zircon, Sm-Nd) analyses performed at the laboratories of IGEM RAS (Moscow), GI KSC RAS (Apatity) and CRPG-CNRS (National Centre for Scientific Research of France, Nancy).

Geological structure. The Monchegorsk ore region is confined to the junction of the Belomorian and Central Kola megablocks and the Imandra-Varzuga zones of Kareliides [2]. The Belomorian megablock lying in the southwestern part of the region comprises tonalite gneisses, amphibolites, migmatites and pegmatites crushed into complex folds as a result of several deformation stages including viscous flow as well as plagiogranites with an age of 2.81 Ga [5]. The Central Kola megablock is composed of rocks of three complexes with an age of 2.83-2.70 Ga [2]. The first complex is represented by oligoclase granites, plagiogranites, and diorites forming dome structures; the second one, by biotite, biotite-amphibole, and sillimanite-garnet gneisses and ferruginous quartzites occurring in inter-dome spaces; the third one is fragmentarily composed of mafic and felsic metavolcanics of the Neoproterozoic greenstone belt. The Imandra-Varzuga zone of Kareliides is represented by a trough-like structure filled with three metavolcanic rock sequences of mafic and intermediate composition separated by layers of tuffaceous sedimentary rocks and quartzites with a total thickness of 2.5-3.0 km. They rest with an angular unconformity on the Archean rocks as well as the eroded surface of the Monchepluton in the area of the Vurechuaivench foothills.

Two large intrusions occur in the central Monchegorsk ore region – the Monchepluton and the Monchetundra massif [3]. The Monchepluton is a typical layered multiphase intrusion composed of mafic-ultramafic rocks. The Monchetundra massif is part of the gabbro-anorthosite complex of the Main Range which separates the Belomorsk and the Central Kola megablocks. In the section of the



Monchetundra massif, gabbro-anorthosites predominate; orthopyroxenites, norites, gabbro-norites, anorthosites as well as gabbro-pegmatites occur in subsidiary amounts. For a long time, the assumption of the Archean age of this complex prevailed [6, 7], but the results of U-Pb dating of zircon and baddeleyite indicate the intrusion of gabbro-anorthosite massifs in the Paleoproterozoic period [3, 8]. In the southern part of the region, chromite-bearing norite-gabbro-norite intrusions of the Imandra-Umbarechensky complex occur, which were emplaced after the start of the Imandra-Varzuga zone formation.

The Monchepluton has an arcuate shape in plan and is composed of two magma chambers [3]. The northern chamber, 7 km long, is oriented to the northeast and shows up as peaks of the Nittis, Kumuzh'ya and Travyanaya mountains (NKT). The southern chamber, 9 km long, extends eastwards from the top of the Sopcha Mountain to Nyud and Poaz mountains (SNP) and further southeastwards to the Vurechuayvench foothills. Each of the chambers has a shape of a symmetrical trough with wings falling at angles of 30-40° (NKT) and from 40-45 to 20-25° with flattening to the axial parts (SNP). Both chambers are tilted to the southwest.

Composite section of the Monchepluton is made up of quartz norites and gabbro-norites of the Basal Zone (BZ) and rocks of five megacycles (macrorhythms), each of them starting with rocks enriched in MgO. Within the Northern Chamber, the following megacycles are distinguished in ascending order: I – harzburgite-orthopyroxenite; II – dunite-harzburgite-orthopyroxenite; within the Southern Chamber: III – dunite-orthopyroxenite-norite; IV – harzburgite-norite-gabbro-norite; V – gabbro-norite-anorthosite. According to the authors of [9], megacycles formed as a result of pulsating intrusion of new portions of magma even prior to complete crystallization of the earlier megacycle. The intrusion of the Monchepluton occurred according to U-Pb dating of zircon in the period of 2507-2498 Ma [3, 8, 10, 11].

In the postintrusive period, during the emplacement of the Imandra-Varzuga zone, the internal structure of the Monchepluton was disturbed by tectonic movements, and rocks of the II megacycle (together with the Sopchezero chromite ore deposit) were lowered relative to the Northern and Southern chambers. The main volume of rocks composing the Monchepluton is not metamorphosed, with the exception of the rocks of the Vurechuayvench foothills, which occur in the western part of the South Chamber and were metamorphosed under conditions of the epidote-amphibolite facies.

For the Monchepluton, two clearly defined trends in the change of contents of the principal rock-forming components have been established [9, 12]. The first trend comprises the series dunites – harzburgites – orthopyroxenites of the I, II and III megacycles which are characterized by a significant increase in SiO₂ content with decreasing MgO. The second trend is the series norites – gabbro-norites – anorthosites of the IV and V megacycles with a significant increase in the Al₂O₃, CaO contents at a relatively stable SiO₂ as MgO decreases. For rocks of all megacycles, the same type of the REE distribution spectra normalized to chondrite were revealed with a slight excess of the LREE over the HREE, but with different degrees of differentiation. A characteristic feature of the rocks of all megacycles is a negative Nb and Ta anomaly and a positive Sr anomaly relative to the depleted mantle (DM).

Monchetundra massif is separated from the Monchepluton by a steeply dipping tectonic zone (Fig.1). This zone is a tectonic mixture of blastocataclasites and blastomylonites after the Archean plagiogneisses and diorites, vein gabbroids and plagiogranites as well as metadolerite dikes cutting them. According to the data on Sm-Nd and Rb-Sr systems, in garnet-amphibole blastocataclasite after gabbro-anorthosite (well M-1, int. 1088.3 m), the fault was emplaced 2.0-1.9 Ga; the temperature reached 620-640 °C, pressure 6.9-7.6 kbar, which corresponds to the amphibolite facies conditions [13].

A significant part of the Monchetundra massif section, deep fault zone and rocks of the Archean basement were penetrated by structural well M-1 with a depth of 2472 m (Fig.1). Rocks of the Lower and Middle zones are also partially penetrated in the Loipishnyun gorge by shallow new wells MT-3, MT-25, MT-69, MT-70 and MT-79 with a depth of 250-355 m [4].



The following zones were distinguished within the central Monchetundra massif: the Lower (well M-1, int. 750-1020 m), the Middle (well M-1, int. 0-750 m) and the Upper (from the mouth of well M-1 to the peaks of the Monchetundra and Hipiknyunchorr, thickness is over 500 m) [3]. The Lower zone has the most heterogeneous composition. Its lower part (908-1020 m) is composed mainly of interbedded gabbro-norites and norites, while the upper one is made up of orthopyroxenites, norites and gabbro-norites. At a depth of 782 and 810 m, thin (about 10 m) harzburgite bodies occur grading at the contacts into melanocratic norites and orthopyroxenites. The Middle zone is composed of trachytoid, mesocratic, less frequently leucocratic gabbro-norites; the Upper zone, of meso- and leucocratic gabbro-norites and anorthosites. Later bodies of coarse-grained gabbro-norites and gabbro-pegmatites occur within all zones.

Composition points of the Monchetundra massif rocks are grouped in petrochemical diagrams in the form of segregated or partially overlapping fields, without forming, in contrast to the Monchepluton, clearly defined trends [9]. Rocks of the Lower zone differ markedly from rocks of the Middle and Upper zones by higher contents of MgO, Cr and low contents of Al₂O₃, CaO; and rock compositions of the Middle and Upper zones largely overlap. All the rocks of the Monchetundra massif are characterized by the same type of flat distribution of the REE spectra normalized to chondrite, a slightly pronounced excess of the LREE over the HREE, and a clear positive Eu anomaly. For them as well as for the Monchepluton, negative Nb and Ta anomalies and a positive Sr anomaly relative to the DM were also established.

Based on generalization of the results of U-Pb isotope analysis of zircon and baddeleyite in rocks of the Monchetundra massif [3, 4, 8], four phases can be distinguished: I (early) – 2521-2516 Ma (distinguished conditionally due to the metamorphic nature of the sampled rocks); II (main), 2507-2496 Ma (mean age 2502±5 Ma, six analyses); III (late) – 2476-2471 Ma (2473 ± 8 Ma, three analyses) and IV (pegmatoid) – 2456-2445 Ma (2451 ± 4 Ma, three analyses). These data indicate that the start of the Monchetundra massif and the Monchepluton intrusion occurred synchronously, but the total duration of their formation differs significantly. According to reconstructions of the *P-T* conditions of the Monchetundra massif and the Monchepluton formation different intervals of rock crystallization temperatures and pressures were determined: *T* = 1190-1000 °C and *P* = 5.3-6.4 kbar for the Lower zone of the Monchetundra massif, *T* = 1300-1200 °C and *P* = 3.0 kbar for the Monchepluton [4]. Thus, the formation of the above intrusions occurred at different depths: of the Monchetundra massif at a depth of about 20 km, and of the Monchepluton, at about 10 km. During the Svecofennian period of orogeny they spatially converged as a result of tectonic movements along the system of deep faults [13].

Samples for isotope studies. For the analysis of U-Pb and Sm-Nd isotope systems, two samples were taken from the core of wells M-1: M-75 (interval 2101-2102 m) and M-77 (interval 911-912 m) (Fig.1).

Sample M-75 weighing 4.9 kg is composed of slightly altered melanocratic olivine gabbro-norite occurring in the upper part of the ultramafic body. Its mineral composition (vol.%) is: olivine 35-40, orthopyroxene 40-45, clinopyroxene 5-10, interstitial basic plagioclase 13-15 partially replaced by chlorite, Cr-spinel as inclusions in olivine and orthopyroxene 2, amphibole 2-3. Rock structure is medium-grained, hypidiomorphic granular, poikilophytic, kelyphitic.

Sample M-77 weighing 8.2 kg was taken from the Lower zone of the Monchetundra massif. It is composed of massive coarse-grained gabbro-norite. Rock structure is poikilophytic, characterized by inclusions of orthopyroxene grains in large prismatic crystals of mafic plagioclase. Clinopyroxene forms grains of subidiomorphic shape to 3-5 mm in size. Small grains of apatite are present. Ore minerals are represented by magnetite and ilmenite. Pyroxene grains are locally replaced by an amphibole aggregate with sulfide microinclusions. At the boundary of orthopyroxene and plagioclase grains, there is a kelyphitic rim of amphibole composition. In its outer part, elongated clinocoesite grains occur. The chemical composition of the sample (wt.%) is: SiO₂ 51.31, TiO₂ 0.28, Al₂O₃ 15.33, Fe₂O₃ 10.94, MgO 9.60, CaO 8.44, Na₂O 2.17, K₂O 0.50, H₂O 1.66, S 0.04.



Analytical methods. Concentration of the main and trace elements in rock samples was determined using the X-ray spectral fluorescence analysis (XRF) on a sequential vacuum spectrometer (with wavelength dispersion), model Axios mAX-Advanced manufactured by PANalytical (Netherlands). The spectrometer is equipped with a 4 kW X-ray tube with an Rh anode. The maximum voltage on the tube is 60 kV, the maximum anode current is 160 mA. When calibrating the spectrometer, branch and national standards, samples of chemical composition of rocks and mineral raw materials were used. Reference samples from the United States Geological Survey (USGS) were used as control samples. The analysis was performed according to the SIMS NSAM procedures, which ensure obtaining results of the III category of accuracy of quantitative analysis according to OST RF 41-08-205-04. The analyses were carried out at the Mineral Substance Analysis Laboratory of the IGEM RAS, analyst A.I. Yakushev. Additionally, the analyses of rocks obtained by ICP-AES and ICP-MS methods (Nancy, France) were made.

Compositions of mineral phases were studied by X-ray spectroscopy using MS-46 CAMECA (GI KSC RAS, Apatity) and CAMECA SX 50 (National Research Centre CRPG-CNRS, Nancy, France).

Zircon populations and rock-forming minerals for U-Pb and Sm-Nd isotope analyses were isolated at the Laboratory of Substance Separation and Primary Sample Processing at the Geological Institute of the KSC RAS under the supervision of L.I. Koval using the standard separation procedure with electromagnets and heavy liquids. The anatomy of zircon crystals in reflected electrons (BSE) and cathodoluminescence (CL) was studied using LEO 1450 scanning electron microscope (Carl Zeiss, Germany) with a Quantax 200 energy dispersive analyzer (Bruker, Germany).

All isotope studies were carried out at the Laboratory of Geochronology and Isotope Geochemistry of the Geological Institute of the KSC RAS. U-Pb zircon dating was performed using the ID-TIMS procedure. Zircon populations subsamples were preliminarily subjected to hydrothermal decomposition in concentrated (48 %) HF acid at a temperature of 205-210 °C for 1-10 days following the method of T. Krogh [14]. Isotope measurements were taken on a Finnigan MAT 262 seven-collector thermal ionization mass spectrometer. Isotope ratios were corrected for mass discrimination obtained by studying parallel analyses of SRM-981 and -982 standards and equal to 0.12 ± 0.04 %. The error in U-Pb ratios was calculated during the statistical calculation of parallel analyses of the IGFM-87 standards and was taken as 0.5 %; if the errors are higher, the real values are given in the table of isotope data. Point coordinates and isochrone parameters were calculated using the ISOPLOT software [15, 16]. Ages were calculated from the accepted values of the decay constants of uranium [17]; errors are given at the level of 2 σ . A correction for the admixture of ordinary Pb was made according to the model [18]. A correction for isotope composition of cogenetic plagioclases was also carried out in cases when the admixture of ordinary Pb exceeded 10 % of the total amount of Pb and $^{206}\text{Pb}/^{204}\text{Pb}$ isotope ratios were less than 1,000. The methodology was described in detail in the work [8].

Measurements of Nd isotope composition and Sm and Nd concentrations were carried out on a Finnigan MAT 262 (RPQ) seven-collector solid-phase mass spectrometer in a static double-filament mode using rhenium and tantalum filaments. The average value of $^{143}\text{Nd}/^{144}\text{Nd}$ ratio in the JNd_i-1 standard over the measurement period was 0.512081 ± 13 (N = 11). The error in $^{147}\text{Sm}/^{144}\text{Nd}$ ratios is 0.3 % (2 σ) – the average value of seven measurements in the BCR-2 standard [19]. Measurement error of Nd isotope composition in an individual analysis is to 0.01 % for minerals with low concentrations of neodymium and samarium. Blank intralaboratory contamination by Nd is 0.3 and Sm – 0.06 ng. Determination accuracy of Sm and Nd concentrations is ± 0.5 %. Isotope ratios were normalized to $^{146}\text{Nd}/^{144}\text{Nd} = 0.7219$ and then recalculated to the table-indicated ratio in the JNd_i-1 standard = 0.512115 [20]. Isochron parameters were calculated using ISOPLOT software [15]. When calculating the $\varepsilon_{\text{Nd}}(T)$ values and model T_{DM} ages modern CHUR values were used after [21] ($^{143}\text{Nd}/^{144}\text{Nd} = 0.512630$, $^{147}\text{Sm}/^{144}\text{Nd} = 0.1960$) and DM after [22, 23] ($^{143}\text{Nd}/^{144}\text{Nd} = 0.513151$, $^{147}\text{Sm}/^{144}\text{Nd} = 0.2136$).



Results of geological, mineralogical, and geochemical studies. Well M-1 crossed at a depth of 2037-2383 m a 340 m thick intrusive body of ultramafic rocks with preserved endocontact chilling zones. Previously, similar rocks were drilled by the well 765 in the interval 1380-1600 m southwest of well M-1 (Fig.1). Proceeding from these data, a conclusion can be drawn on the displacement (lowering) of the ultramafic body penetrated by the well M-1 relative to the fragment exposed by the well C-765 as well as its wedging out in the southwestern direction and a sheet-lenticular shape. The body is separated from the lower contact of the Monchetundra massif by a fault zone over one kilometer thick (Fig. 1). It has a clear intrusive relationship with the enclosing rocks of the Archean diorite complex exerting a pronounced thermal effect on them with formation of hornfels. At contacts with the enclosing rocks, rocks of endocontact chilling zones were found, their grain size ranging from small to fine when approaching the contacts. The upper zone about 10 m thick (of which 6.6 m are fine-grained) is composed of melanocratic norite; and the lower zone about 37 m thick (of which 2.5 m are fine-grained) is composed of orthopyroxenite.

Composition of minerals is given in Table 1; rock composition including the contents of the principal components, ore, trace, and rare earth elements, in Tables 2, 3.

The main volume of the intrusive body is filled with plagioharzburgite. It differs from harzburgite of the Monchepluton North Chamber by the presence of interstitial mafic plagioclase and a minor admixture of clinopyroxene. Rock structure is hypidiomorphic-granular, poikilitic. Mineral composition of plagioharzburgite (vol.%) is: 65-85 olivine (86.8-88.4 % Fo), 10-25 orthopyroxene (Fs = 11.2-12.6 %), 6-15 plagioclase (43-53 % An), 3-5 augite ($f = 10-13$) and 1-3 Cr-spinel (Table 1). Olivine contains an admixture of NiO (0.09-0.62 %), Cr-spinel – TiO₂ (0.22-0.71; 2.38 %), ZnO (0.10-0.73 %) and NiO (0.10-0.72 %). The composition of rock-forming minerals varies slightly through the section. One can note a slight increase in Fs in orthopyroxene when approaching the contacts of the body. At the olivine/plagioclase boundary, there is a single-layer kelyphitic reaction rim composed of a cross-fibrous amphibole aggregate. Plagioclase is partly replaced by chlorite.

Table 1

Composition of minerals from rocks of well M-1 based on microprobe analysis, wt.%

Depth, m	SiO ₂	TiO ₂	Cr ₂ O ₃	CaO	Al ₂ O ₃	FeO	MnO	MgO	Na ₂ O	K ₂ O	ZnO	NiO	Sum	Index
Olivine														Fo, %
2145	40.04	0.30	–	–	–	12.33	0.68	45.83	–	–	–	0.17	99.34	86.9
2326.5	40.93	–	0.31	–	–	12.39	0.09	46.34	–	–	0.03	0.09	100.17	86.9
2326.5	41.06	–	–	–	–	12.13	0.19	46.76	–	–	–	0.35	100.50	87.3
2326.5	41.13	–	–	–	–	12.49	0.22	46.27	–	–	0.04	0.39	100.54	86.8
2350.5	41.10	0.02	0.09	–	–	11.03	0.09	47.13	–	–	0.04	0.62	100.10	88.4
2350.5	41.04	0.04	–	–	–	11.03	0.11	46.95	–	–	–	0.60	99.77	83.5
Orthopyroxene														Fs, %
2145	55.745	0.258	0.207	1.118	0.919	8.026	0.129	32.569	–	–	–	0.753	99.724	11.3
2326.5	54.726	–	0.327	0.963	1.422	8.682	0.164	32.581	–	–	–	0.091	98.956	12.0
2326.5	55.510	–	0.276	1.299	1.610	8.775	0.205	32.450	–	–	–	0.091	100.216	12.6
2350.5	56.238	0.222	0.621	0.302	1.339	8.120	0.114	32.845	–	–	0.029	0.181	100.011	11.7
2350.5	56.311	0.094	0.397	0.452	1.484	7.927	0.095	32.595	–	–	0.038	0.166	99.559	11.5
Plagioclase														An, %
2145	53.490	–	–	11.140	27.422	0.618	–	–	6.345	0.054	–	–	99.069	49.1
2145	54.010	–	–	11.060	27.122	0.051	–	–	6.707	0.043	–	–	98.993	47.6
Cr-spinel														Mg#
2145	0.385	–	45.053	–	12.424	33.176	–	4.908	–	–	0.381	0.11	96.437	25.94
2188.8	0.066	0.650	41.145	–	12.826	33.79	0.574	6.473	–	–	0.295	0.095	95.914	33.67
2188.8	0.117	0.708	42.432	–	13.602	31.662	0.601	6.827	–	–	0.219	0.047	96.215	35.11
2326.5	0.665	2.384	35.271	–	14.346	35.035	0.641	6.745	–	–	0.162	0.111	95.360	33.58
2326.5	–	0.225	35.717	–	13.926	37.536	0.500	7.003	–	–	0.477	0.095	95.479	36.64
2350.5	0.442	0.284	39.977	–	16.153	30.647	0.351	7.097	–	–	0.409	0.330	95.690	36.91
2350.5	0.559	0.341	41.939	–	14.910	29.574	0.364	7.007	–	–	0.143	0.362	95.199	36.63
2350.5	–	0.235	42.003	–	17.566	29.238	0.364	6.303	–	–	0.257	0.723	96.689	32.65

Note. Fo – forsterite, mol.%, Fs – ferrosilite, mol.%, An – anorthite, mol.%, Mg# = 100×Mg/Mg + Fe (a.p.f.u).



Table 2

Composition of rocks from well M-1 based on XRF data, wt.%, ppm

Components	Depth, m												
	2037.4	2096.7	2153.2	2167.3	2196.5	2216.2	2239	2285.5	2302	2318.8	2339.3	2351.3	2383.3
SiO ₂	52.89	41.62	41.39	40.83	40.9	40.67	40.56	40.5	40.96	42.3	43.85	49.53	49.33
Al ₂ O ₃	7.72	4.11	3.63	3.32	3.30	2.78	3.14	2.55	3.34	3.22	3.03	4.57	8.77
TiO ₂	0.30	0.18	0.15	0.17	0.12	0.12	0.16	0.12	0.14	0.14	0.13	0.12	0.33
Fe ₂ O _{3tot}	8.50	11.18	10.88	11.05	10.78	11.09	11.14	10.64	10.45	10.24	10.05	9.67	10.85
MnO	0.15	0.15	0.14	0.15	0.14	0.15	0.15	0.14	0.14	0.14	0.145	0.15	0.17
MgO	22.94	36.87	38.92	39.55	39.93	41.05	40.08	41.85	39.9	39.3	37.87	31.45	19.83
CaO	5.04	2.75	2.20	2.28	1.72	1.53	2.09	1.38	2.02	1.98	2.29	2.45	6.68
Na ₂ O	1.12	0.56	0.63	0.58	0.49	0.45	0.54	0.39	0.40	0.52	0.47	0.59	1.38
K ₂ O	0.12	0.24	0.13	0.17	0.10	0.14	0.17	0.15	0.13	0.13	0.08	0.09	0.29
i.l.	0.37	0.61	0.01	0.01	0.44	0.01	0.01	0.24	0.63	0.17	0.35	0.01	1.60
Sum	99.15	98.27	98.08	98.11	97.92	97.99	98.04	97.96	98.11	98.14	98.26	98.63	99.23
Cr	3566	8722	9718	9390	10698	10246	9826	10266	9285	9260	8764	6997	2892
Ni	815	2274	2507	2585	2630	2729	2675	2733	2604	2465	2149	1469	778

Note. 2037.4, 2383.3 – rocks of chilling zones; the rest, plagiolarzburgites; i.l. – ignition loss.

Table 3

Composition of rocks from well M-1 based on ICP-AES and ICP-MS, ppm

Components	Depth, m					Components	Depth, m				
	2043.6	2052.2	2128.8	2272.0	2373.8		2043.6	2052.2	2128.8	2272.0	2373.8
SiO ₂	54.65	46.13	43.14	41.91	50.90	Y	4.77	4.58	3.46	3.20	7.27
Al ₂ O ₃	5.41	5.52	4.25	3.00	8.96	Zr	13.41	11.91	10.00	12.99	23.69
TiO ₂	0.20	0.20	0.16	0.15	0.30	Nb	0.18	0.24	0.24	0.58	0.62
Fe ₂ O _{3tot}	7.99	10.85	10.79	10.28	10.43	Ba	75.82	88.99	74.79	71.22	167.44
MnO	0.14	0.18	0.17	0.16	0.16	La	3.25	3.70	3.24	3.34	6.94
MgO	26.70	32.25	37.14	40.87	20.75	Ce	6.94	7.91	6.41	7.15	14.26
CaO	3.96	3.80	2.58	1.70	6.18	Pr	0.91	1.06	0.86	0.95	1.81
Na ₂ O	0.75	0.84	0.67	0.31	1.44	Nd	3.95	4.35	3.49	3.90	7.43
K ₂ O	0.06	0.11	0.08	0.24	0.37	Sm	0.85	1.00	0.74	0.76	1.52
P ₂ O ₅	0.09	0.09	0.09	0.10	0.10	Eu	0.27	0.29	0.25	0.19	0.47
i.l.	0.01	0.01	0.28	0.74	0.48	Gd	0.75	0.86	0.61	0.60	1.32
Sum	99.96	99.98	99.35	99.46	100.07	Tb	0.12	0.13	0.10	0.10	0.21
V	96.06	86.00	73.65	63.11	126.14	Dy	0.79	0.72	0.60	0.56	1.18
Co	70.24	109.95	124.92	133.21	89.59	Ho	0.15	0.17	0.13	0.13	0.24
Ni	1045.0	1933.0	2479.0	2822.0	810.88	Er	0.51	0.46	0.32	0.32	0.77
Cu	102.90	45.73	20.71	13.69	44.74	Tm	0.08	0.08	0.05	0.05	0.10
Pb	1.64	1.40	1.14	1.20	2.31	Yb	0.47	0.49	0.34	0.34	0.72
Zn	54.39	80.26	79.86	76.14	79.18	Lu	0.09	0.09	0.06	0.05	0.11
Rb	1.97	2.94	2.49	9.05	10.70	Hf	0.44	0.35	0.26	0.32	0.70
Sr	86.58	100.43	80.41	48.44	166.17	Ta	0.02	0.02	0.01	0.04	0.04
						Th	0.18	0.21	0.16	0.49	0.35

Note. Fe₂O_{3tot} = FeO + 0.9 Fe₂O₃.

Melanocratic norite is the last member in the series of endocontact rocks: plagiolarzburgite – orthopyroxenite – melanonorite connected by gradual transitions. Mineral composition of melanonorite (vol.%) is: 40-70 orthopyroxene ($f = 12-14\%$), 25-40 plagioclase (51-56 % An), 5-10 augite ($f = 10-13\%$), 0.5-1 Cr-spinel and <1 sulfides.

Vertical section of the investigated body (Fig.2) reflects variations in the principal (SiO₂, Al₂O₃, Fe₂O_{3tot}) and ore (Cr, Ni) components. The section clearly shows a symmetrical distribution of the contents of rock-forming components associated with a decrease in MgO, Cr and Ni and an increase in SiO₂ and Al₂O₃ towards both contacts. This feature is in good agreement with the distribution of crystallization temperature, which is stable in the main volume of the body and decreasing at the contacts. There is a slight increase in MgO content in the lower and of Al₂O₃ content in the upper parts of the massif, which is associated with minor shows of the accumulation of olivine and

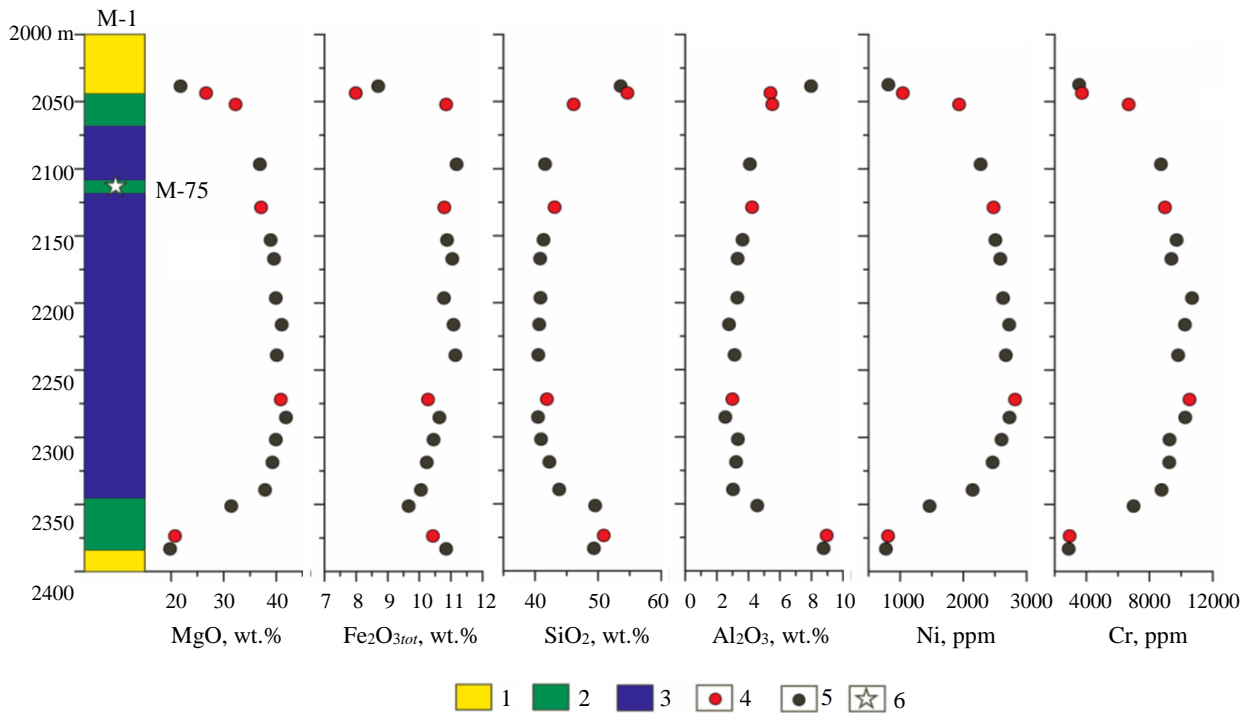


Fig.2. Schematic section of the ultramafic rock body penetrated by well M-1 (int. 2,037-2,337 m) and variations of the contents of rock-forming and ore components in rocks, wt.%, ppm

1 – host rocks of the hypersthene diorite complex; 2 – melanonorites and orthopyroxenites of chilling zones; 3 – plagiolarzburgites; 4 – according to ICP-AES (CRPC-CMRS) data; 5 – according to XRF (IGEM RAS) data; 6 – location of M-75 sample

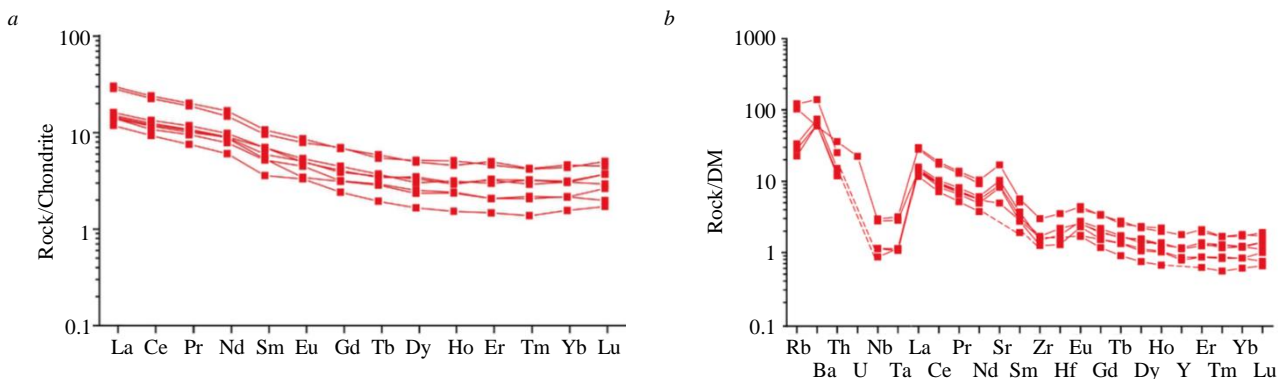


Fig.3. REE distribution spectra in rocks of the ultramafic body (a) normalized to chondrite [24], and spider diagrams (b) normalized to DM after [22]

plagioclase, respectively. Fe_2O_{3tot} shows a slight increase up the section and a disturbance of the trends near the contacts. The first is associated with a gradual decrease of crystallization temperature, and the second – with a relatively abrupt cooling of melt at the contacts. For Nd, a uniform distribution was established over most of the section within 3.49-4.35 ppm and an increase in its content to 7.43 ppm near the lower contact (Table 2).

Rocks that make up the studied massif are characterized by the same type of the REE distribution spectra normalized to chondrite, with a slight excess of the LREE over the HREE and a minor degree of differentiation (Fig.3).

Their characteristic feature is a negative Nb- and Ta-anomaly and a positive Sr-relative to DM (Fig.4). Compared to the rocks of the Monchetundra massif, they lack a positive Eu-anomaly. Judging by the REE spectra and spider diagrams, rocks of the sheet body show the greatest similarity with rocks of the South Chamber of the Monchepluton [9].

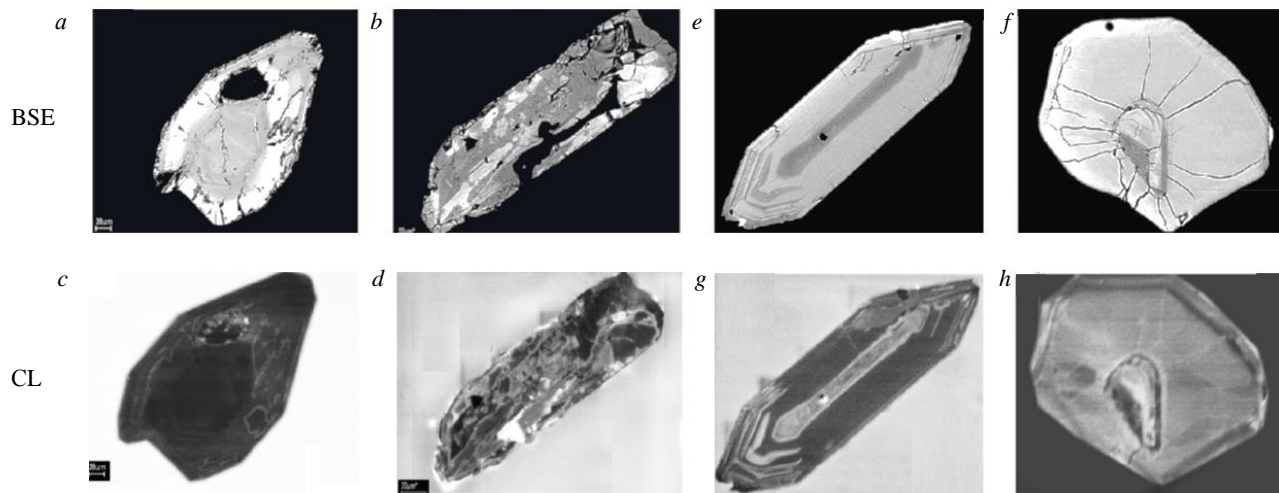


Fig.4. Photomicrographs of zircon grains from samples M-75 (a-d) and M-77 (e-h) taken in reflected electron (BSE) and cathodoluminescence (CL) modes

Results of isotope studies. Sample M-75. Zircon monofraction (0.50 mg) was divided into four populations. *The first* of them is represented by fragments of large crystals. Their average size is 0.175×0.175 mm (Ec – 1). Light yellow colour, vitreous lustre, slightly corroded surface. Minor zoning is recorded in the marginal zone. Grains contain a fine network of microcracks; the marginal zone is fissured. *Zircon population 2* – short prismatic crystals with well-defined pyramid and pinacoid faces and slightly rounded edges (Fig.4, a, c). Their average size is 0.175×0.175 mm (Ec – 1). Crystals are limpid, light yellow, with vitreous lustre. The surface is not corroded. Crystals contain a large nucleus with coarse zoning. Cracks are radiating from the nucleus. In the wide marginal part, a primary oscillation rhythmic zoning of magmatic type is recorded. *Zircon population 3* is represented by small fragments of crystals of various shapes. Their average size is 0.170×0.170 mm (Ec – 1). Grains are limpid, light yellow with a vitreous lustre. *Zircon population 4* contains elongated prismatic, intensely cracked crystals (Fig.4, b, d). Their average size is 0.24×0.105 mm (Ec – 2.2). Milky colour, vitreous lustre. In BSE and CL, intraphase heterogeneity was recorded due to the processes of post-intrusive metamorphic alterations. The results of U-Pb isotope analysis of zircon are presented in Table 4.

Table 4

Results of U-Pb isotope analysis of zircon from olivine melanocratic (M-75) and coarse-grained (M-77) gabbro-norites

N	Weight, mg	Concentration, ppm		Isotope composition of lead			Isotope ratios and age, Ma			Rho
		Pb	U	$^{206}\text{Pb}/^{204}\text{Pb}$	$^{206}\text{Pb}/^{207}\text{Pb}$	$^{206}\text{Pb}/^{208}\text{Pb}$	$^{207}\text{Pb}/^{235}\text{U}$	$^{206}\text{Pb}/^{238}\text{U}$	$^{207}\text{Pb}/^{206}\text{Pb}$	
Magmatic zircon M-75										
1	0.10	365.75	524.58	977	4.7720	1.7623	9.76278	0.431079	2500	0.99
2	0.20	95.98	168.93	6247	5.8814	2.2971	9.23281	0.409738	2508	0.92
3	0.10	211.83	335.50	828	5.3433	1.5995	8.84685	0.392795	2491	0.89
Xenogenic zircon M-75										
4	0.10	28.19	35.16	1171	5.1455	2.1929	14.1301	0.536971	2789	0.97
Magmatic zircon M-77										
1	0.40	153.45	478.32	4404	6.3914	5.5386	9.17510	0.420551	2436	0.93
2	0.10	435.73	797.9	1359	6.0709	1.6570	7.58804	0.354236	2406	0.95
3	0.10	209.05	400.5	1866	6.0811	1.5646	7.10140	0.332917	2431	0.83
4	0.40	374.48	926.2	3114	6.4656	1.8958	5.76009	0.277478	2352	0.96

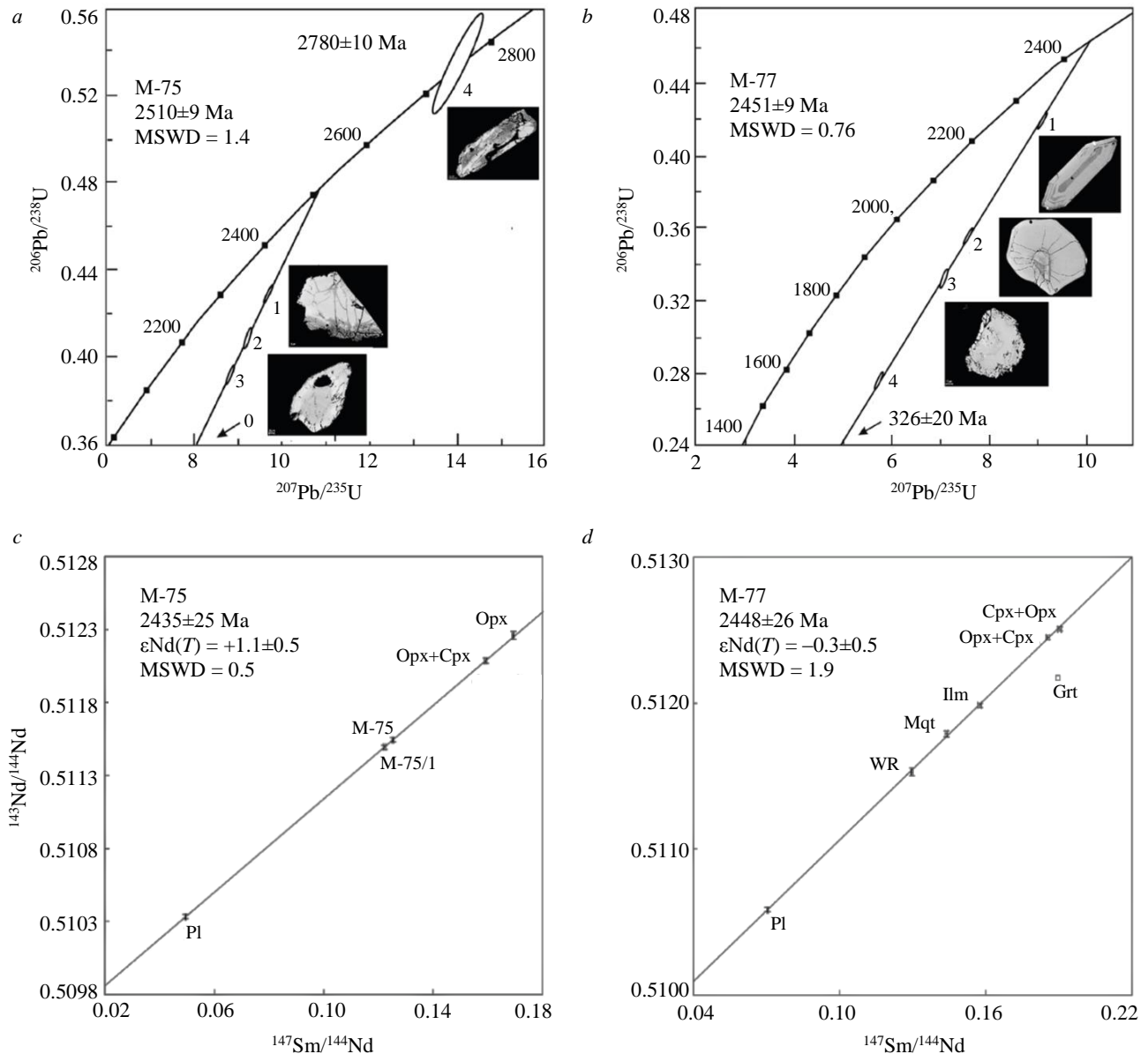


Fig.5. U-Pb diagrams with concordia for zircon (a, b) and mineral Sm-Nd isochrone (c, d) for melanocratic olivine (M-75) and coarse-grained (M-77) gabbroanorthites
WR, M-75, M-75/1 – sample; Pl – plagioclase; Opx – orthopyroxene; Cpx – clinopyroxene; Mgt – magnetite; Ilm – ilmenite

On the U-Pb diagram with concordia (Fig.5, a), analytical points of zircon populations 1, 2, and 3 are approximated by discordia with an upper intersection at 2510 ± 9 Ma (MSWD = 1.4); the lower intersection equal to zero reflects the current Pb losses. Analytical point for population 4 lies on concordia with an age of 2780 ± 10 Ma. Based on the shape of grains, their internal structure and the results of U-Pb isotope analysis, populations 1, 2, and 3 are combined into a morphological type which characterizes zircon of magmatic genesis; population 4 should be assigned to the metamorphosed type. They differ markedly in U content (169-524 and 35 ppm). The result obtained, 2510 ± 9 Ma, coincides, within the analytical error, with the age of magmatic zircon and baddeleyite from intrusive rocks of the Monchepluton (2507-2498, average 2502 ± 5 Ma) [3, 10, 11, 8]. The age of 2780 ± 10 characterizes the metamorphism of xenogenic zircon which corresponds in age to one of the metamorphic stages of granite gneisses from the basement of the Monchegorsk ore region.

Sample M-77. Zircon monofraction weighing 1.0 mg is divided into four populations. *Population 1* is represented by crystals of an elongated prismatic and dipyrmidal habit (see Fig.4, e, g). Crystals are



transparent, light yellow with a vitreous lustre, the surface is not corroded. The average dimensions are 0.175×0.06 (Ec – 2.9). Weight of an average crystal is $25.2 \cdot 10^{-6}$ g. Crystals contain a nucleus of dipyrnidal prismatic habit with a weakly pronounced intraphase inhomogeneity. The main part of the crystal has a well-defined primary oscillation magmatic zoning parallel to the outer faces. *Population 2* contains lamellar fragments of crystals. Grains are limpid, light yellow with a greasy lustre; the surface is slightly corroded. Their average dimensions are 0.175×0.105 (Ec – 1.6). Weight of an average crystal is $7.7 \cdot 10^{-6}$ g. Grains contain an internal seed of an oval irregular shape with fine rhythmic zoning. In the outer thin rim, a thin rhythmic growth zoning was also recorded. *Population 3* is represented by fragments of semi-oval crystals. The average grain size is 0.140×0.105 (Ec – 1.3). Weight of an average crystal is $6.1 \cdot 10^{-6}$ g. Grains are transparent, yellowish-brown with a greasy lustre; the surface is corroded. Outer zone is cracked. Grains contain a polygonal nucleus slightly expressed in BSE and CL with an intraphase inhomogeneity. There are relics of a thin rim. *Population 4* contains fragments of zircon crystals of indefinite shape with minor inclusions (baddeleyite?). Grains are limpid, light yellow with a vitreous lustre. The surface is not corroded. The average grain size is 0.140×0.105 (Ec – 1.3). Weight of an average crystal is $6.1 \cdot 10^{-6}$ g.

Grain shapes, their internal structure reflecting the growth processes in magmatic melt and the results of U-Pb isotope analysis of populations 1-4 characterize zircon of magmatic genesis. U content in this zircon varies from 400 to 926 ppm (Table 4), which is comparable with zircon from gabbro-norites in the Middle zone of the Monchetundra massif [3].

On the U-Pb diagram with concordia, the analytical points for four populations of zircon from sample M-77 are approximated by discordia with the upper intersection at 2451 ± 9 Ma (MSWD = 0.76) (Fig.5, b). The lower intersection at 326 ± 20 Ma corresponds to the emplacement stage of major alkaline syenite intrusions (Khibiny, etc.). The age of 2451 ± 9 Ma does not coincide with the age of zircon from norites (2500 ± 2 Ma) and orthopyroxenites ($2,496 \pm 3$ Ma) occurring within the Lower zone of the Monchetundra massif [4] but corresponds to the age of zircon from rocks of the IV Postintrusive pegmatoid phase that are cutting rocks of the Middle and Upper zones of the Monchetundra massif (2456-2445 Ma). These results testify to a heterogeneous structure of the Lower zone of the Monchetundra massif which comprises rocks aged from 2500 to 2450 Ma.

The results of Sm-Nd studies of samples M-75 and M-77 are presented in Table 5. For M-75, the sample, plagioclase and pyroxene subsamples were measured; for M-77, the sample, pyroxene, magnetite, and ilmenite subsamples were measured. The samples differ in Nd content in silicates and rock – 3.70-4.77 and 5.13-6.83 ppm, respectively.

Table 5

Results of isotope Sm-Nd analysis of samples M-75 and M-77

Subsample	Concentration, ppm		Isotope ratios		T_{DM} , Ma	$\epsilon_{Nd}(T)$
	Sm	Nd	$^{147}\text{Sm}/^{144}\text{Nd}$	$^{143}\text{Nd}/^{144}\text{Nd}$		
M-75						
WR-1	0.858	4.14	0.1253	0.511542 ± 18	2762	+0.9
WR-2	0.747	3.70	0.1222	0.511493 ± 8	2749	+0.9
Pl	0.391	4.77	0.0495	0.510332 ± 12		
Opx	0.536	1.914	0.1692	0.512259 ± 13		
Opx+Cpx	1.685	6.40	0.1591	0.512085 ± 11		
M-77						
WR	1.099	5.13	0.1296	0.511529 ± 28	2925	-0.3
Pl	0.752	6.46	0.0704	0.510585 ± 12		
Cpx+Opx	2.149	6.83	0.1902	0.512507 ± 11		
Opx+Cpx	1.893	6.17	0.1854	0.512451 ± 14		
Mgt	0.725	3.05	0.1437	0.511791 ± 18		
Ilm	1.930	7.41	0.1574	0.511985 ± 15		
Gr	1.053	3.38	0.1886	0.512221 ± 9		

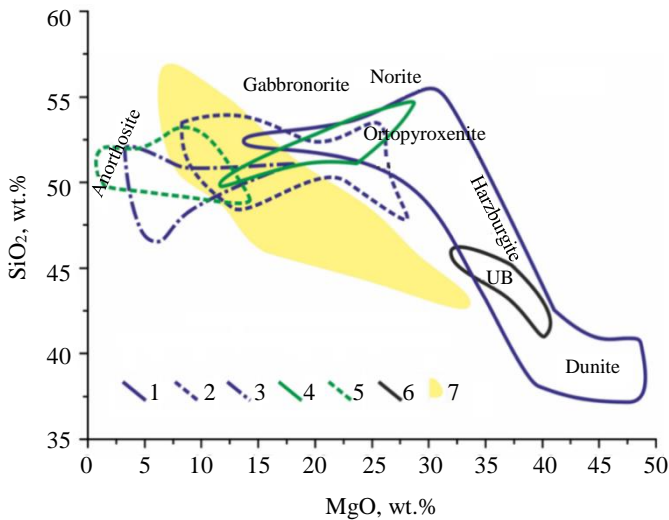


Fig.6. Petrochemical SiO₂-MgO diagram with fields of rock composition of ultramafic body (well M-1), the Monchepluton and Monchetundra massif

- 1-3 – rocks I-III (1), IV (2) and V (3) of the Monchepluton megacycles;
 4-5 – rocks of the Lower (4), Middle and Upper (5) zones of the Monchetundra massif; 6 – ultramafic body (UB);
 7 – komatiitic basalts of the Vetreny Belt after [25, 26]

also not a younger intrusion, since the age of its emplacement coincides with the age of the Monchepluton and the beginning of the Monchetundra massif formation. By its structure, the investigated body is an independent intrusive massif with preserved chilling zones and a slightly manifested intrachamber differentiation. These data allow assigning it to the fragment of a magma feeding system in the form of a paleochannel through which ultramafic magma could enter the overlying magma chamber.

MgO-SiO₂ diagram (Fig.6) displays the composition fields of plagioharzburgites of the magma paleochannel and rocks of the Monchepluton (I-V megacycles), the Monchetundra massif (three zones) as well as komatiitic-basalts from the Vetreny Belt with an age of 2.41 Ga. In this diagram, plagioharzburgites of the paleochannel fall into the field of the Monchepluton harzburgites differing from them by higher contents of Al₂O₃ and CaO (twofold) at the same MgO content [9]. The diagram also reflects clear differences in differentiation in komatiitic basalts volcanics which are assigned to comagmatic formations of layered intrusions [25, 26] and in the Monchepluton. The differences in differentiation trends are due to the fact that crystallization of the olivine phase played the main role in volcanic rocks, while in the Monchepluton and other layered intrusions of the Paleoproterozoic age in the region, a more complex grading of olivine-chromite and olivine-orthopyroxene paragenesis into orthopyroxene-plagioclase paragenesis occurred. A complicating factor is the repeated flow of melts differing in composition and mineralization into the magma chamber.

$\epsilon_{Nd}-T$ (Ma) diagram (Fig.7) plotted from the results of Sm-Nd analysis displays the data on the rocks of the paleochannel as well as the Monchepluton and Monchetundra massif with correction of the age of rocks according to the U-Pb analysis of zircon and baddeleyite. Most of analytical points lie in the area of negative values of the ϵ_{Nd} parameter, which is typical for most of the layered ore-bearing intrusions of Paleoproterozoic age in the Kola-Lapland-Karelian province [8, 27, 28]. This feature, according to the authors of [3, 29], is due to the processes of assimilation and contamination of highly metamorphosed host rocks in deep and intermediate chambers within the lower and middle crust.

For olivine gabbronorite (sample M-75), an isochron age of 2435 ± 25 Ma was obtained, MSWD = 0.5 (Fig.5, c). It differs from the U-Pb age of zircon, apparently, due to local alteration of plagioclase. For coarse-grained gabbronorite (sample M-77), the isochron age is 2448 ± 26 Ma, MSWD = 1.9 (Fig.5, d). It coincides within the analytical error with the U-Pb age of zircon. For sample M-75, a positive value of ϵ_{Nd} (+1.1) parameter was determined; for sample M-77, it is negative (-0.3). Samples also differ in model age of the original magma protolith: 2.75 and 2.92 Ga respectively.

Discussion. The studied intrusive body of ultramafic rocks intersected by well M-1 is separated from the Monchetundra massif by a thick zone of blastocataclasites and blastomylonites and, therefore, cannot be included in its composition. The body is



Positive values of the ϵ_{Nd} parameter established for rocks of the paleochannel (+1.1), dunite and chromitite of the Sopcheozero deposit of the Monchepluton (+2.5 and +2.9) and orthopyroxenite from the Lower zone of the Monchetundra massif (+1.7), whose age is within 2510-2496 Ma (average 2501 ± 6 Ma), deserve special attention. These data point to the occurrence of rocks with mantle marks, which represent slightly contaminated mantle matter in the investigated rock massifs. From this an assumption about the supply of magmas from different deep or intermediate chambers and about an incomplete homogenization of magmas in the magma chamber follows. This conclusion allows to account for the occurrence in the Monchepluton of deposits of different metallogeny – chromite and sulfide Cu-Ni ores. The data obtained also indicate that thin bodies of ultramafic rocks occurring within the Lower zone of the Monchetundra massif [3, 4] are independent magma injections. Apparently, they are also the product of the common magma feeding system, which was in the junction area of the Monchepluton and the Monchetundra massif.

Conclusions. The 340 m thick lenticular-sheet body of plagioclase-bearing gabbros occurring at a depth of about 2.2 km is a fragment of a magma feeding system in the form of a paleochannel, through which high-magnesium magma ascended into the overlying magma chamber. Rocks of the investigated body are quite similar in mineral composition, geochemical and isotope features to rocks of the Monchepluton, which is a classic example of a layered ore-bearing intrusion. The intrusion age determined from U-Pb isotope analysis of zircon (ID-TIMS) is 2510 ± 9 Ma, which is comparable to the period of the Monchepluton formation. The studied geological body is a unique example of a magma feeding system for an ore-bearing layered intrusion of Precambrian age.

The authors are grateful to Daniel Ohnenstetter and Evgeniy Sharkov for their assistance in the analytical work and to the reviewers for their constructive comments.

REFERENCES

1. Sharkov E.V. Petrology of Layered Intrusions. Leningrad: Nauka, 1980, p. 184 (in Russian).
2. Mitrofanov F.P., Pozhilenko V.I., Arzamastsev A. et al. Geology of the Kola Peninsula (Baltic Shield). Apatity: Kola Science Center RAS, 1995, p. 144.
3. Layered intrusions of the Monchegorsk Ore Region: Petrology. Mineralization. Isotopy. Deep Structure / Eds.: F.P.Mitrofanov, V.F.Smolkin. Apatity: Izd-vo Kolskogo nauchnogo tsentra RAN, 2004. Part 1, p. 177; Part 2, p. 177 (in Russian).
4. Chashchin V.V., Bayanova T.B., Savchenko Y.E. et al. Petrogenesis and Age of Rocks from the Lower Zone of the Monchetundra Mafic Platinum-Bearing Massif. Kola Peninsula. *Petrology*. 2020. Vol. 28. N 2, p. 151-182. DOI: 10.1134/S0869591120020022
5. Vetrin V.R. Composition and Structure of the Lower Crust of the Belomorian Mobile Belt. Baltic Shield. *Petrology*. 2006. Vol. 14. N 4, p. 390-412. DOI: 10.1134/S0869591106040047
6. Kozlov E.K. Natural Rock Series of Nickel-Bearing Intrusions and Their Metallogeny. Leningrad: Nauka, 1973, p. 283 (in Russian).
7. Yudin B.A. Gabbro-Labradorite Formation of the Kola Peninsula and its Metallogeny. Leningrad: Nauka, 1980, p. 169 (in Russian).
8. Bayanova T., Mitrofanov F., Serov P. et al. Layered PGE Paleoproterozoic (LIP) Intrusions in the N-E Part of the Fennoscandian Shield – isotope Nd-Sr and $3\text{He}/4\text{He}$ data. Summarizing U-Pb Ages (on Baddeleyite and Zircon). Sm-Nd Data (on Rock-Forming and Sulphide Minerals). Duration and Mineralization. Geochronology – Methods and Case Studies. Chapter 6. INTECH. 2014, p. 143-193. DOI: 10.5772/58835

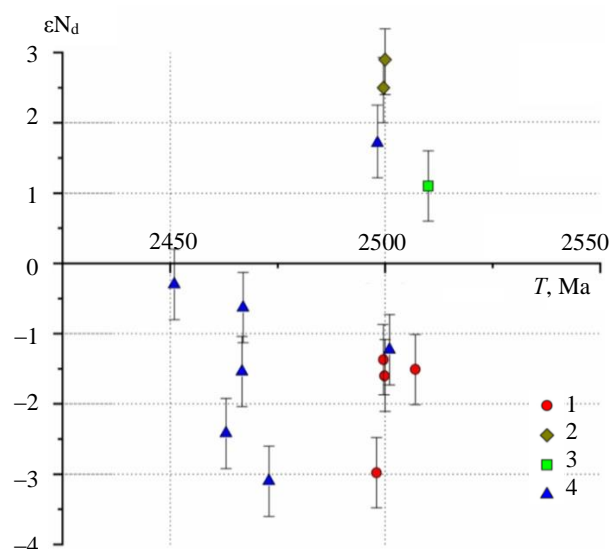


Fig.7. Primary $\epsilon_{Nd}(T)$ ratio in rocks of the ultramafic body of Monchepluton and Monchetundra massif relative to age (T , Ma)

1 – the Monchepluton; 2 – dunite and chromitite of Sopcheozero deposit; 3 – ultramafic rocks; 4 – Monche-, Chuna- and Volchjatundra massifs.

Data used: 1 – [3, 8, 27, 28]; 2 – [10]; 3 – present work; 4 – [3, 4, 8]. Age is corrected from the results of U-Pb isotope analysis of zircon [3, 7, 8, present work]



9. Smolkin V.F., Mokrushin A.V. Geochemistry of Paleoproterozoic Layered Intrusions of the Monchegorsk Ore Region. Kola Region. Trudy XVI Fersmanovskoi nauchnoi sessii GI KNTs RAN. 7-10 aprelya 2019, Apatity. Rossiya. Apatity: Izd-vo Kol'skogo nauchnogo tsentra RAN, 2019. N 16, p. 544-549 (in Russian). DOI: 10.31241/FNS.2019.16.111
10. Chashchin V.V., Bayanova T.B. Sopchezero Chromium Deposit of the Monchepluton: Geochemistry and U-Pb Age. Trudy XVIII Fersmanovskoi nauchnoi sessii GI KNTs RAN. 5-6 aprelya 2021. Apatity. 2021. Apatity: Izd-vo GI KNTs RAN, 2021. N 18, p. 403-408 (in Russian).
11. Amelin Yu.V., Heaman L.M., Semenov V.S. U-Pb geochronology of layered mafic intrusions in the eastern Baltic Shield: implications for the timing and duration of Paleoproterozoic continental rifting. *Precambrian Research*. 1995. Vol. 75. Iss. 1-2, p. 31-46. DOI: 10.1016/0301-9268(95)00015-W
12. Karykowski B.T., Maier W.D., Groshev N.Y. Critical Controls on the Formation of Contact-Style PGE-Ni-Cu Mineralization: Evidence from the Paleoproterozoic Monchegorsk Complex. Kola Region. Russia. *Economic Geology*. 2018. Vol. 113. N 4, p. 911-935. DOI: 10.5382/econgeo.2018.4576
13. Sharkov E.V., Chistyakov A.V., Smolkin V.F. et al. Age of the Moncha Tundra Fault. Kola Peninsula: Evidence from the Sm-Nd and Rb-Sr Isotopic Systematics of Metamorphic Assemblages. *Geochemistry International*. 2006. Vol. 44. N 4, p. 317-326. DOI: 10.1134/S001670290604001X
14. Krogh T.E. A low-contamination method for hydrothermal dissolution of zircon and extraction of U and Pb for isotopic age determinations. *Geochimica et Cosmochimica Acta*. 1973. Vol. 37. Iss. 3, p. 485-494. DOI: 10.1016/0016-7037(73)90213-5
15. Ludwig K.R. ISOPLOT/Ex – A geochronological toolkit for Microsoft Excel. Version 2.05. Berkeley Geochronology Center Special Publication. N 1a. 1999, p. 49.
16. Ludwig K.R. PBDAT – A Computer Program for Processing Pb-U-Th isotope Data. Version 1.22. Open-file report 88-542. US Geological Survey. 1991, p. 38.
17. Steiger R.H., Jager E. Subcommittee on geochronology: Convention on the use of decay constants in geo- and cosmochronology. *Earth and Planetary Science Letters*. 1977. Vol. 36. Iss. 3, p. 359-362. DOI: 10.1016/0012-821X(77)90060-7
18. Stacey J.S., Kramers J.D. Approximation of terrestrial lead isotope evolution by a two-stage model. *Earth and Planetary Science Letters*. 1975. Vol. 26. Iss. 2, p. 207-221. DOI: 10.1016/0012-821X(75)90088-6
19. Raczek I., Jochum K.P., Hofmann A.W. Neodymium and strontium isotope data for USGS reference materials BCR-1, BCR-2, BHV O-1, BHVO-2, AGV-1, AGV-2, GSP-1, GSP-2 and Eight MPI-DING reference glasses. *Geostandards and Geoanalytical Research*. 2003. Vol. 27, p. 173-179. DOI: 10.1111/j.1751-908X.2003.tb00644.x
20. Tanaka T., Togashi S., Kamioka H. et al. JNdi-1: A neodymium isotopic reference in consistency with LaJolla neodymium. *Chemical Geology*. 2000. Vol. 168, p. 279-281. DOI: 10.1016/S0009-2541(00)00198-4
21. Bouvier A., Vervoort J.D., Patchett P.J. The Lu-Hf and Sm-Nd isotopic composition of CHUR: Constraints from unequilibrated chondrites and implications for the bulk composition of terrestrial planets. *Earth and Planetary Science Letters*. 2008. Vol. 273. Iss. 1-2, p. 48-57. DOI: 10.1016/j.epsl.2008.06.010
22. Salters U.J.M., Stracke A. Composition of the depleted mantle. *Geochemistry. Geophysics. Geosystems*. 2004. Vol. 5. Iss. 5, p. 1-27. DOI: 10.1029/2003GC000597
23. Goldstein S.J., Jacobsen S.B. Nd and Sr isotopic systematics of river water suspended material: implications for crustal evolution. *Earth and Planetary Science Letters*. 1988. Vol. 87. Iss. 3, p. 249-265. DOI: 10.1016/0012-821X(88)90013-1
24. McDonough W.F., Sun S.S. The composition of the Earth. *Chemical Geology*. 1995. Vol. 120. Iss. 3-4, p. 222-253. DOI: 10.1016/0009-2541(94)00140-4
25. Evseeva K.A., Krassivskaya I.S., Chistykov A.V., Sharkov E.V. The Early Paleoproterozoic Boninite-Like Volcanics from the Vetreny Belt. Southeastern Baltic Shield. Russia. *Lithosphere (Russia)*. 2004. Vol. 3, p. 110-126 (in Russian).
26. Mezhelovskaya S.V., Korsakov A.K., Mezhelovskii A.D., Bibikova E.V. Age range of formation of sedimentary-volcanogenic complex of the Vetreny Belt (the southeast of the Baltic Shield). *Stratigraphy and Geological Correlation*. 2020. Vol. 24, p. 105-117. DOI: 10.1134/S0869593816020040
27. Amelin Yu.V., Semenov V.S. Nd and Sr isotope geochemistry of mafic layered intrusions in the eastern Baltic Shield: implications for the evolution of Paleoproterozoic continental mafic magmas. *Contributions to Mineralogy and Petrology*. 1996. Vol. 124, p. 255-272. DOI: 10.1007/s004100050190
28. Serov P.A. Paleoproterozoic Pt-Pd Fedorovo-Pansky and Cu-Ni-Cr Monchegorsk Ore Complexes: Age, Metamorphism, and Crustal Contamination According to Sm-Nd Data. *Minerals*. 2021. Vol. 11. Iss. 12. N 1410. DOI: 10.3390/min11121410
29. Smolkin V.F., Kremetskii A.A., Vetrin V.R. Geological and Geochemical Model of Emplacement of Paleoproterozoic (2.5-2.4 Ga) Ore Magmatic Systems of the Baltic Shield. *Otechestvennaya geologiya*. 2009. N 3, p. 54-62 (in Russian).

Authors: Valeriy F. Smolkin, Doctor of Geological and Mineralogical Sciences, v.smolkin@sgm, <https://orcid.org/0000-0002-1400-6310> (Vernadsky State Geological Museum, Russian Academy of Sciences, Moscow, Russia), Artem V. Mokrushin, Candidate of Geological and Mineralogical Sciences, Senior Researcher, <https://orcid.org/0000-0002-5586-8902> (Geological Institute of the Kola Science Centre, Russian Academy of Sciences, Apatity, Russia), Tamara B. Bayanova, Doctor of Geological and Mineralogical Sciences, Chief Researcher, <https://orcid.org/0000-0001-7281-8707> (Geological Institute of the Kola Science Centre, Russian Academy of Sciences, Apatity, Russia), Pavel A. Serov, Candidate of Geological and Mineralogical Sciences, Leading Researcher, <https://orcid.org/0000-0003-0930-0301> (Geological Institute of the Kola Science Centre, Russian Academy of Sciences, Apatity, Russia), Aleksey A. Ariskin, Doctor of Geological and Mineralogical Sciences, Professor, <https://orcid.org/0000-0002-5081-2731> (Lomonosov Moscow State University, Moscow, Russia).

The authors declare no conflict of interests.